Hysteresis of the Water Retention Curve in Recycled Aggregates Concrete: Comparison of Experimental and Numerical Approaches

Arthur Fanara[a,b,*], Luc Courard[a], Frédéric Collin[a]

[a] *Urban and Environmental Engineering, University of Liege, Belgium*
[b] *FNRS-F.R.I.A, Fonds de la Recherche Scientifique, Belgium*

Abstract

The effects of the water retention curve hysteresis on concrete made from Recycled Concrete Aggregates are investigated. A multiscale multiphase FE^2 model is developed and validated experimentally. Properties for the calibration of the hysteresis are also obtained experimentally. A coupled chemo-hydraulic multiscale model, able to represent the chloride ingress inside the porous structure of concrete, was developed with the Finite Element squared (FE^2) method. The constitutive equations are based on properties that are measured in laboratory conditions, for concrete manufactured with 100% Natural Aggregates (NA) or Recycled Concrete Aggregates (RCA), respectively. The hysteresis of the water retention curve is implemented according to the Van Genuchten formulation. Results suggest that not accounting for the hysteresis of the water retention curve introduces a significative error in the saturation degree of concrete and, therefore, in the chloride content.

Keywords: Hysteresis, Water Retention Curves, Degradation, Durability, Finite Element Analysis, Microstructure, Multiscale Modelling, Recycled Aggregates, Transport Properties, Waste Management

*Corresponding author.
Email addresses: arthur.fanara@uliege.be (Arthur Fanara), luc.courard@uliege.be (Luc Courard), f.collin@uliege.be (Frédéric Collin)

1. Introduction

Durability of concrete can be defined as the ability of a structural concrete member to withstand the effect of time and degradation processes while retaining its strength for which it was designed [1]. Degradation processes can have multiple causes such as freeze-thaw cycles, carbonation, chloride attacks or, in most cases, a combination of these [2, 3]. Most of the degradation processes that take place in concrete depend on the water content of the concrete porous system. For freeze-thaw cycles, the greater the saturation degree of the material is and the greater the degradation may be. For chloride attacks and carbonation, corrosive ions require water to migrate and reach the reinforcements [4]. Furthermore, reactions of corrosion are the most critical at around 85% of saturation degree [5]. Understanding the transfer of water in concrete is therefore crucial for the evaluation of its durability.

In spite of the environmental concerns related to concrete manufacturing, the use of recycling materials is being promoted as substitute to natural materials. Recycled Concrete Aggregates (RCA) have thus been studied for many years to reduce the consumption of Natural Aggregates (NA). Unfortunately, this substitution tends to decrease the durability properties of concrete, mainly due to changes in its porous structure [6, 7, 8]. This modification of the porous system is then correlated to differences in the water transfer properties of concrete. An extensive study of water transfer properties must then be performed in order to better apprehend the effects of that substitution on durability [8].

The water content of many geomaterials, such as concrete, has been characterised through Water Retention Curves (WRC) in the literature [9, 10, 11, 12, 13, 8]. Water retention curves relate the degree of saturation of a porous medium to the environmental conditions such as the relative humidity and the temperature, through the expression of the total suction. For this definition to be valid, the theory of porous media must be applied to the porous system of concrete. That is, pores of concrete can only be filled of air, water or a mix of both. In a saturated porous medium, the pores are filled with water, whereas in an unsaturated porous medium, the porous system is filled with both water and air. The theory of mixture [14, 15] is also applied to concrete. It states that all phases are assumed to occupy the same region of space simultaneously, as the superposition of different continua. It allows the mass balance equations of our model to be defined for each phase separately [14], with interactions between the constituents [15].

The total suction can be written through the Kelvin's law:

$$s = -\rho_w \frac{R\,T}{M} \ln(RH) \tag{1}$$

with s the matrix suction [Pa], ρ_w the water density [kg/m^3], R the constant of ideal gases (equal to 8.3143 [J/K.mol]), M the molar mass of water (equal to 18.016 [g/mol]) and, finally, T and RH the temperature [K] and Relative Humidity [-], respectively. In this paper, we make the assumption that the total suction is equal to a matrix suction, that is to the difference between the air pressure and the water pressure:

$$s = P_g - P_w \tag{2}$$

with P_g and P_w the gas and water pressures [Pa], respectively.

An example of WRC is given in Figure 1. The shape of the WRC depends significantly on the porous structure of the material [11, 16], and four zones are often depicted, depending on the number of phases filling the pore system and the (dis)continuous nature of said phases [11]:

1. When the suction is smaller than the air-entry pressure (denoted as α in Figure 1), then the material is completely saturated, as no air can enter the pores and therefore, no water can escape. This section is almost horizontal, and some authors refer to it as the boundary effect zone due to the local exchanges between the surface of the sample and its environment [11, 17, 16];
2. Once the suction is equal to the air-entry pressure, air can enter the porous system and the degree of water saturation decreases. This state is called the funicular state where the liquid phase is continuous and the gas phase consists of isolated air pockets.

This section marks the transition from the funicular state (which consisted of the first two sections) to the pendular state (that is the last two sections) [11, 17, 16];

3. The third section is defined by discontinuous gas and liquid phases, neither being continuous anymore. It is also part of the transition zone [16];
4. The last region observed is the residual state [16, 11], where the water saturation degree is equal to the residual saturation degree, often noted $S_{r,res}$. It corresponds to the water content that may never be extracted without extreme heating, such as chemically bonded water.

A porous material such as concrete exhibits two separate water retention curves: one specific for drying conditions, and another one for wetting conditions, the shape of both curves being modelled as similar. Depending on the drying and wetting history of the porous material, the water retention curve can follow an infinity of paths [11]: this is the hysteresis phenomenon. It is often associated to multiple causes:

- The ink-bottle effect [9, 10, 19, 16, 20]: the cross section of the pores are irregular, requiring a local increase in suction for the liquid phase to continue its movement. The water content inside a capillary is indeed different at drying or wetting, at equal suction;

- The raindrop effect [9, 10, 19, 16, 20]: the value of the contact angle is different between an advancing and a receding meniscus;

- Entrapped air [21, 10, 22, 19, 16, 20]: the liquid phase is required to push the air out of the porous medium prior to rewetting, which can lead to entrapped air inside the material, accounting for up to 10% of the volume of a soil [10].

The hysteresis phenomenon is presented in Figure 2. The two main WRC, that is the boundary drying curve and the boundary wetting curve, act as limits that may never be crossed. In between, an infinity of scanning curves can be created, depending on the history of the material [9, 19].

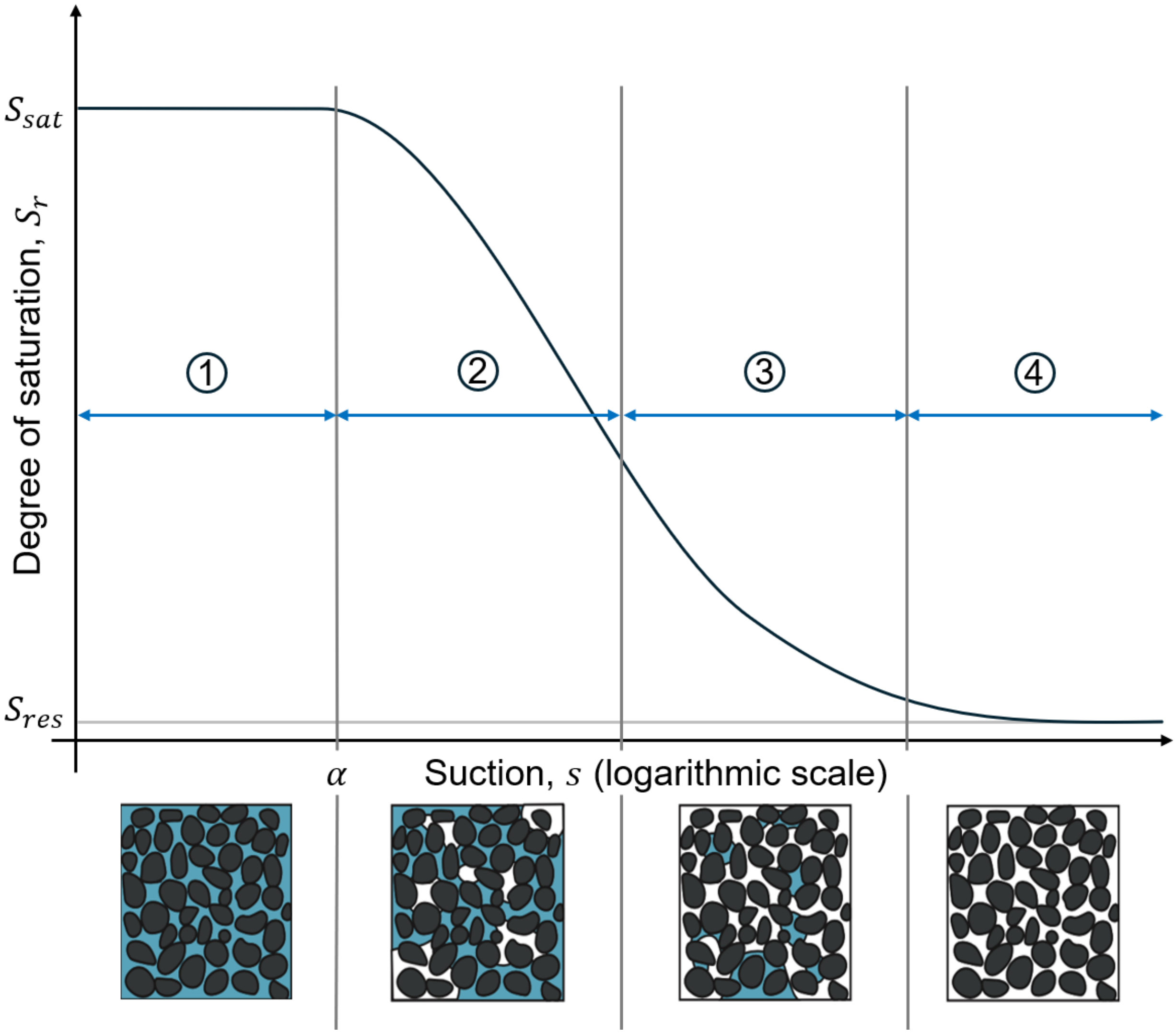

Figure 1: Typical water retention curve (modified after [11, 18])

The scientific community has developed many models to represent the water retention curve of geomaterials. They can be divided into two categories: the domain models (also called physically based models) and the empirical models [10, 22]. Amongst the domain models, some are called dependent models or independent models [23], depending on whether the model takes into account the water content of surrounding pores or not, respectively [10]. The domain models, in general, represent the porous system of a material as a collection of pore domains of specific radii, based on the domain theory of capillary hysteresis [22, 10]. In that theory, the pores can only be full of water or empty, each state being assigned to a

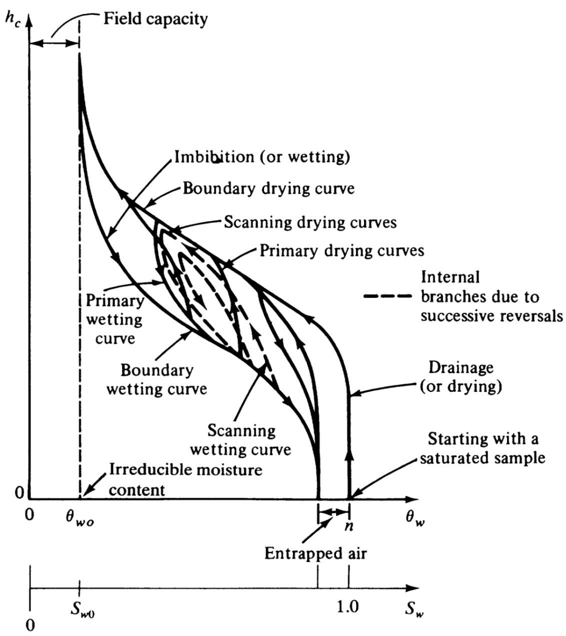

Figure 2: Hysteresis in the water retention curve (from [9])

value of drying or wetting suction [10]. On the other hand, the empirical models focused on the development of empirical laws that were fitted to experimental results [10, 24]. For the empirical models, two subgroups can be observed [10]: those that use the same empirical equation for both boundary drying and wetting curves, adjusting the value of the fitting parameters accordingly [24], and those that express relationships between the two curves. An extensive comparison of 29 models based on experimental results for 34 soils has been presented in Pham et al. (2005) [10]. Unfortunately, no data is available for similar experiments on concrete.

The description of the hysteresis is often neglected in numerical models, as the validation of such models require experimental results, that are often hard to obtain and very time consuming. Furthermore, it increases the number of parameters describing the WRC. Hence no consensus was found in the litterature on the incorporation of the hysteresis inside numerical models [22].

For this research, as the durability of concrete greatly depends on the saturation degree of its porous system, it was decided to implement the hysteresis of the water retention curve. Experimental results allowed the precise determination of the numerous parameters required for the model. To better quantify the effect of the hysteresis on durability, the model also incorporates the ingress of chloride ions, which can serve as an indicator of durability inside reinforced concrete. Furthermore, this work is part of a study that tends to characterise the influence of the substitution of natural aggregates with recycled concrete aggregates inside concrete. A comparison of the hysteresis effect between the two materials is also presented.

2. Materials and Methods

2.1. Materials

The experimental phase of this work focused on obtaining intrinsic properties for the transfer of water and chlorides inside several materials:

- a concrete made from Natural Aggregates (NA), called Natural Aggregates Concrete (NAC), that comprises CEM I 42.5 N cement, 0/2 Rhine Sand and 2/7 limestone aggregates;
- a concrete made from Recycled Concrete Aggregates (RCA), called Recycled Aggregates Concrete (RAC), that comprises the same cement and sand than the NAC but with 2/7 RCA. The RCA originate from another study made at the University of Liège named SeRaMCo [25]. They consist of sandstone concrete blocks cast in the laboratory and crushed multiple times by an impact crusher. The particle size distribution of the RCA was reconstructed to be similar to that of the NA, and the substitution was performed with a 100% substitution ratio at equal volume;
- an equivalent mortar, called E-M, composed of the same cement and Rhine sand than the two concretes, and whose composition method was the Concrete Equivalent Mortar method [26].

The composition and fresh properties of the three materials defined are visible in Table 1, and more information on the materials may be found in Fanara et al. (2023) [27].

Table 1: Composition and fresh properties of the materials characterised: NAC, RAC and E-M.

Composition	m_{agg} (kg/m^3)	m_{sand}	m_{cement}	m_{water}	W/C	Efficient W/C
NAC	1111	643	320	172.5	0.54	0.5
RAC	946	643	320	201.2	0.63	0.5
E-M	-	1337	622.5	336	0.54	0.54

2.2. Methods

The experiments performed were aimed at determining water transfer properties or chloride transfer properties:

- Water transfer properties [8]:
    - the water absorption, dry and saturated densities, and water-accessible porosity of our materials were determined according to the ASTM C 642-97 "Standard Test Method for Density, Absorption, and Voids in Hardened Concrete";
    - the water intrinsic permeability was obtained according to the NBN EN ISO 17892-11:2019;
    - the parameters of the water retention curves were obtained with the vapour control method. This experiment is detailed in Section 2.2.1 below.
- Chloride transfer properties [27]:
    - the chloride diffusion coefficient was obtained with an experiment of chloride diffusion under transient conditions, following the guidelines of the NBN EN 12390-11 "Testing hardened concrete - Part 11: Determination of the chloride resistance of concrete, unidirectional diffusion".

2.2.1. Static Sorption and Desorption

The Water Retention Curve can be obtained by fitting an empirical model, such as the one of Van Genuchten (1980) [24] to experimental results. Experimentally, the water saturation degree of a material may be linked to the suction through the expression of the Kelvin's law (Equation 1). To obtain our boundary drying and wetting curves, the vapour control method is implemented [28], based on the hypothesis that all hygroscopic materials absorb or release water vapour depending on their water saturation degree, in order to reach equilibrium with the humid air they are in contact with: the vapour pressure and temperature inside the porous system and outside must be equal [28]. The control of the relative humidity of the ambient medium, through the use of saline solutions, and the control of the temperature through a climatic chamber, enable the acquisition of several (s ; S_r) points on the water retention curves [29, 13]. The saline solutions and their respective target suction at 21°C are shown in Table 2.

Table 2: Saline solution and their respective target RH [%] and suction [MPa] at 21°C, used for the determination of the water retention curves of our materials.

Saline Solution	KCl	NaCl	$Ca(NO_3)_2$	$MgCl_2$	Silica salt
Target RH [%]	90	75	56	35	6
Target Suction [MPa]	-14.3	-39.1	-78.7	-142.5	-381

Samples are initially saturated, or dried at 105°C, until they reach a constant mass. Then, they are placed inside a chamber with one of the saline solutions. Each week, the mass and the ambient air parameters (RH and T) are measured. After approximately three months, the sample mass doesn't vary considerably anymore and the sample is considered in equilibrium. Based on its mass at equilibrium and previous measurements of its dry and saturated mass, the degree of saturation can be obtained. To model the hysteresis, the samples were put in a first chamber, then after hygroscopic equilibrium and measurement of their mass, they were changed of chamber. This was repeated multiple times to obtain a noticeable hysteresis.

2.2.2. Modelling the Water Retention Curve hysteresis

The model implemented in this work is the empirical model of Van Genuchten (1980) [24] for the boundary curves, and the model of Zhou et al. (2012) [30] for the hysteresis curves.

According to Van Genuchten, the water saturation degree is linked to the suction through the following equation [24]:

$$S_e = S_{res} + (S_{sat} - S_{res}) \left(1 + \left(\frac{s}{\alpha}\right)^n\right)^{-m} \text{ with } m = 1 - \frac{1}{n} \tag{3}$$

where n [-] is an adimensional model parameter related to the rate of desaturation of the soil and m [-] is another adimensional model parameter related to the curvature (slope) of the water retention curve. The last model parameter, denoted α [Pa], is related to the air-entry pressure [8]. Finally, one can see the maximum saturation degree S_{sat} [-] and the residual saturation degree S_{res} [-] [17], as well as the suction s [Pa].

The main boundary curves of the water retention curves, defined by Equation 3, can be written specifically for the drying curve (with a suffix d) and for the wetting curve (with the suffix w):

$$S_{e,w} = S_{res} + (S_{sat} - S_{res}) \left[1 + \left(\frac{s}{\alpha_w}\right)^{n_w}\right]^{-m_w} \tag{4}$$

$$S_{e,d} = S_{res} + (S_{sat} - S_{res}) \left[1 + \left(\frac{s}{\alpha_d}\right)^{n_d}\right]^{-m_d} \tag{5}$$

The scanning curve (suffix s) is then defined by [30]:

$$\frac{\partial S_{e,s}}{\partial s}(\text{wetting}) = \left(\frac{s_w}{s}\right)^b \left(\frac{\partial S_{e,w}}{\partial s}\right) \text{ with } s_w = \alpha_w \left(S_e^{-1/m_w}\right)^{1/n_w} \tag{6}$$

$$\frac{\partial S_{e,s}}{\partial s}(\text{drying}) = \left(\frac{s_d}{s}\right)^{-b} \left(\frac{\partial S_{e,d}}{\partial s}\right) \text{ with } s_d = \alpha_d \left(S_e^{-1/m_d}\right)^{1/n_d} \tag{7}$$

where the parameter b [-] is defined as a fitting parameter, always positive. It influences the gradient of the scanning curve: the closer it gets to zero and the closer the hysteresis curve is to the main curve, while the greater it is and the more horizontal the hysteresis curve gets [30]. The wetting and wetting boundary curves, along with an example of a scanning curve, are shown in Figure 3.

The final saturation degree may then be obtained thanks to the derivative defined above and the increment of suction (ds) applied:

$$S_e^t = S_e^{t-1} + \left(\frac{\partial S_{e,s}}{\partial s}\right) \times ds \tag{8}$$

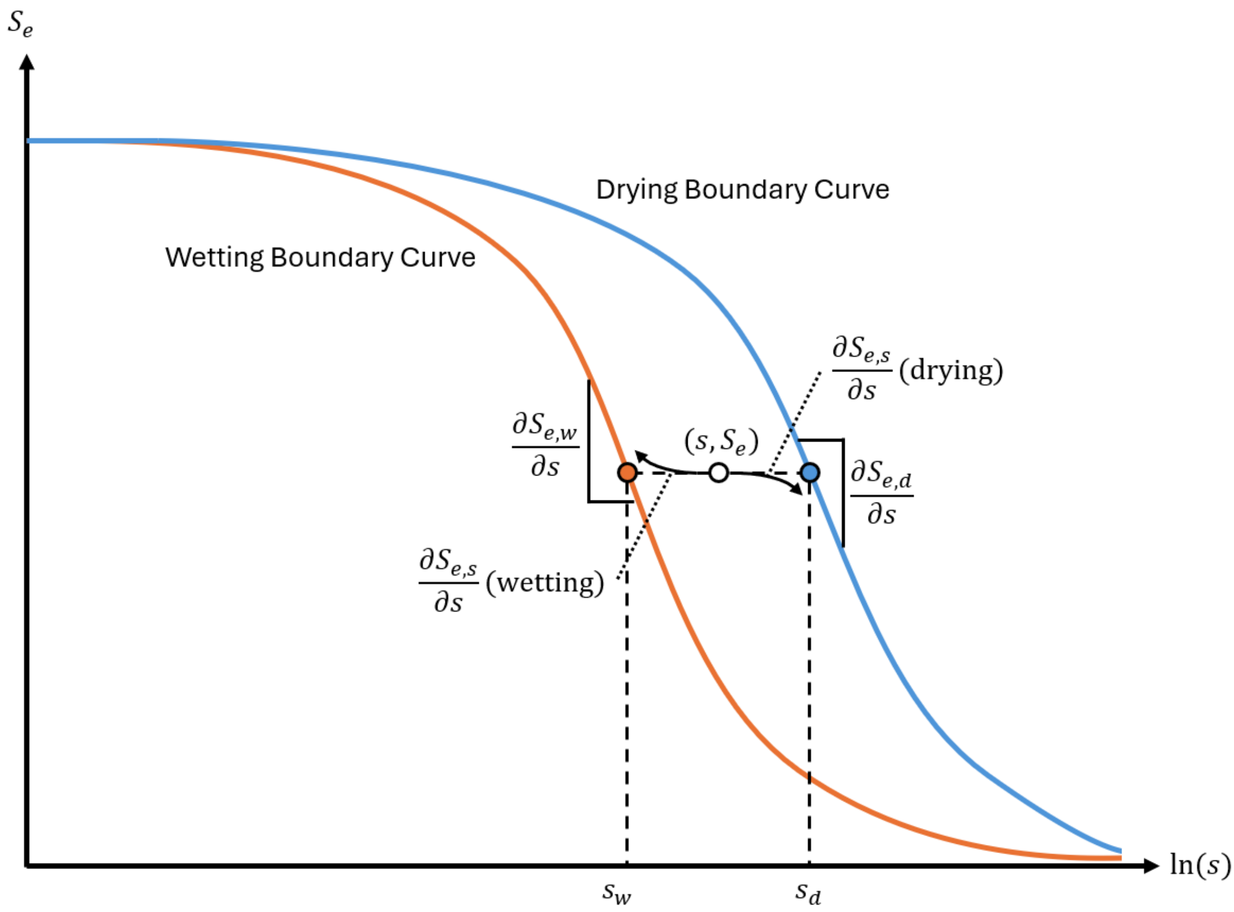

Figure 3: Drying/wetting boundary and scanning curves (modified after [30]).

It is clear from this formulation that the increment of suction plays an important role in the accuracy of the results, as the scanning curve is obtained from the slope, at a given suction, of the main boundary curve.

The experimental results with the WRC fitted with the Van Genuchten model are shown in Figures 4, 5 and 6 for the NAC, RAC and E-M, respectively. In blue is represented the boundary drying curve and in orange the boundary wetting curve. The experimental data is shown with markers and their error bars. The Van Genuchten model is proven to accurately fit the experimental data of our materials.

In Figure 7 are shown the results for the hysteresis part of this experiment. Two sets of hysteresis were measured. The samples were initially dry: they adsorbed water along the boundary wetting curve, then the hysteresis started with 3 desaturation steps followed by a final re-saturation phase. The model by Zhou et al. (2012) was then fitted based on the parameters of the boundary curves obtained previously. Each hysteresis resulted in a different values for the fitting parameter b, with a small difference between the minimal ($b = 0.75$) and maximal ($b = 1.2$) values found.

A summary of the properties obtained is visible at Table 3. The parameter n_{vG} is rather constant for a specific composition, and the difference in between compositions is not that important. For the parameter α_{vG}, which is related to the air-entry pressure, the greater the maximum pore size of the porous material and the smaller it is in desorption. It is therefore logical that a mortar has a smaller air-entry pressure than concretes, and that the RAC has a greater maximum pore size than the NAC. The inverse is true for the sorption.

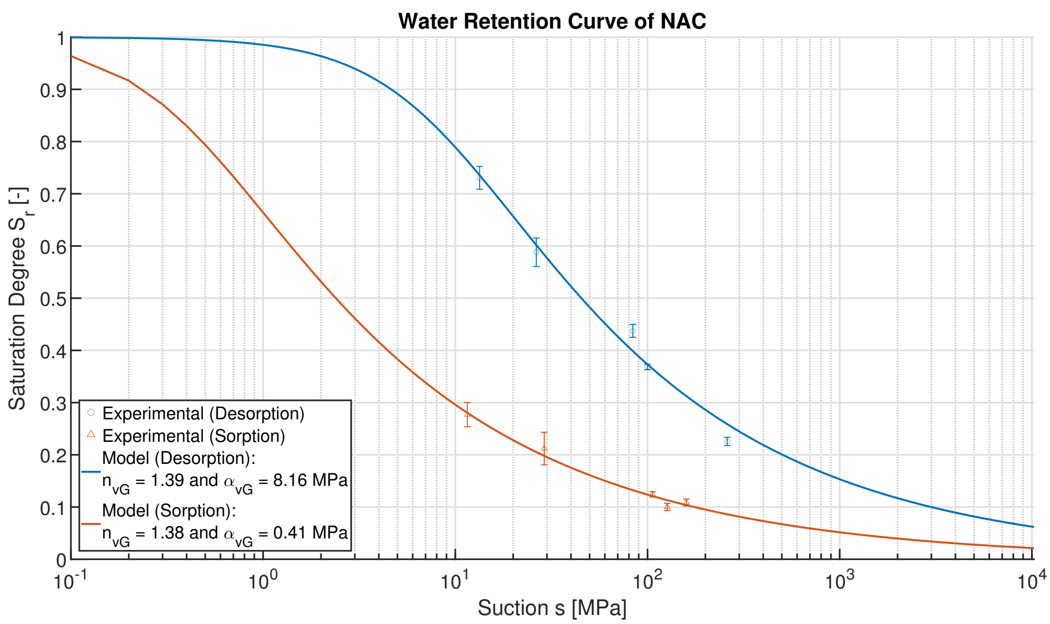

Figure 4: Water Retention Curve of the NAC obtained by fitting the Van Genuchten model to the experimental results of the sorption and desorption experiment.

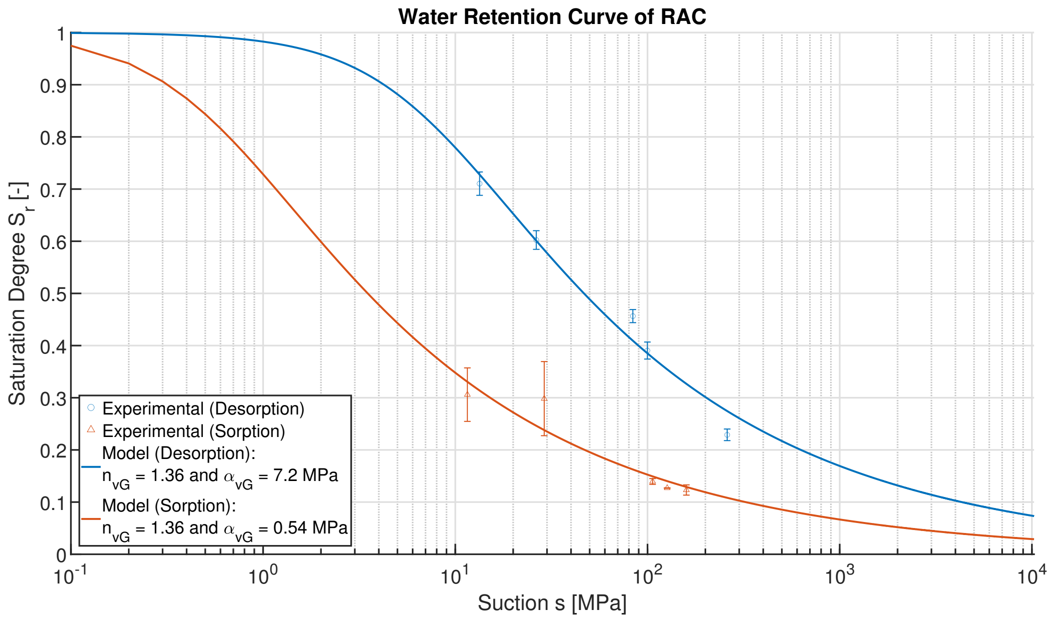

Figure 5: Water Retention Curve of the RAC obtained by fitting the Van Genuchten model to the experimental results of the sorption and desorption experiment.

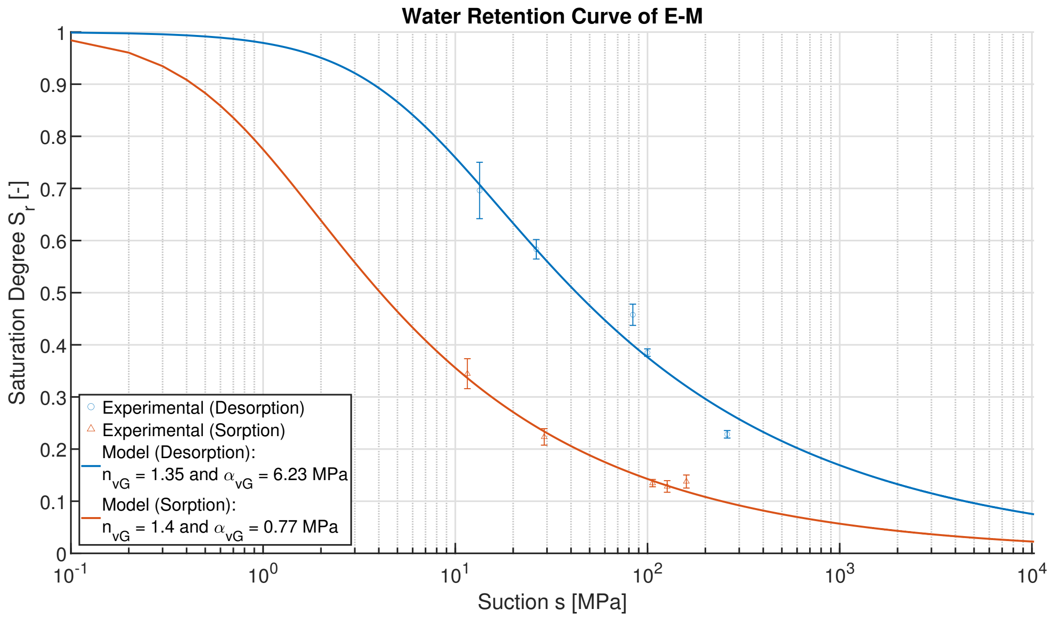

Figure 6: Water Retention Curve of the E-M obtained by fitting the Van Genuchten model to the experimental results of the sorption and desorption experiment.

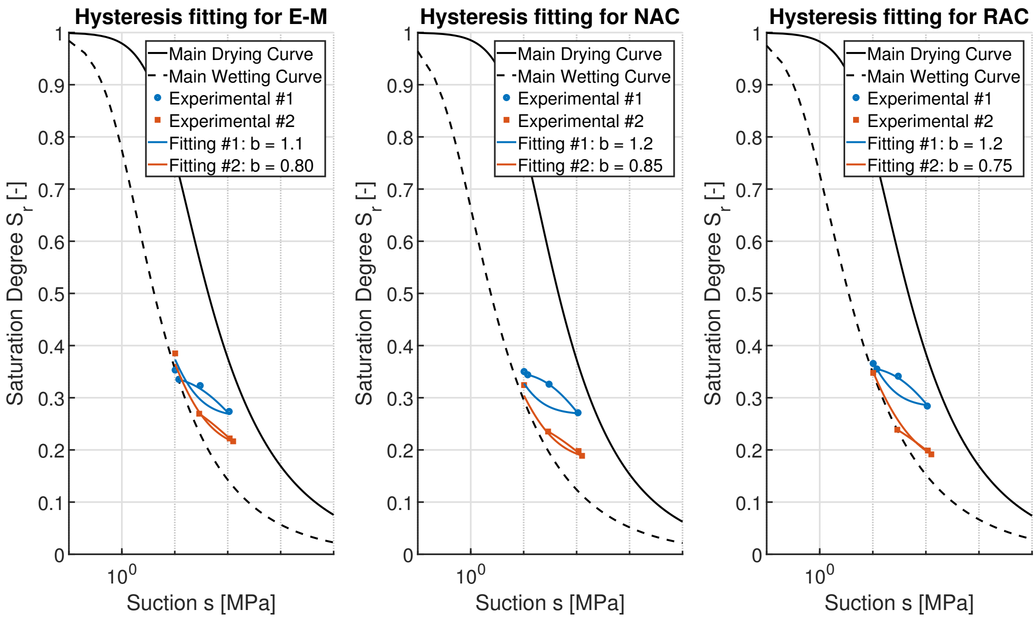

Figure 7: Fitting of the hysteresis of the WRC for all three compositions based on the model by Zhou et al. (2012) [30].

3. Numerical Model

The numerical model implemented for this work is a multiscale multiphase model based on the Finite Element Squared (FE^2) method. It is implemented in the FE software LAGAMINE [31] developed at the University of Liège.
The multiscale model allows the modelling of water and gas flows, as well as chloride ions diffusion and advection, inside a saturated or unsaturated porous material, with the subscale representing a slice of concrete made of mortar (either new mortar or adherent mortar for the RCA) and impervious natural aggregates, as represented in Figure 8.
The model has been proven to be able to replicate experimental results of a concrete based on intrinsic properties of a mortar, the subscale filling the gap [32].

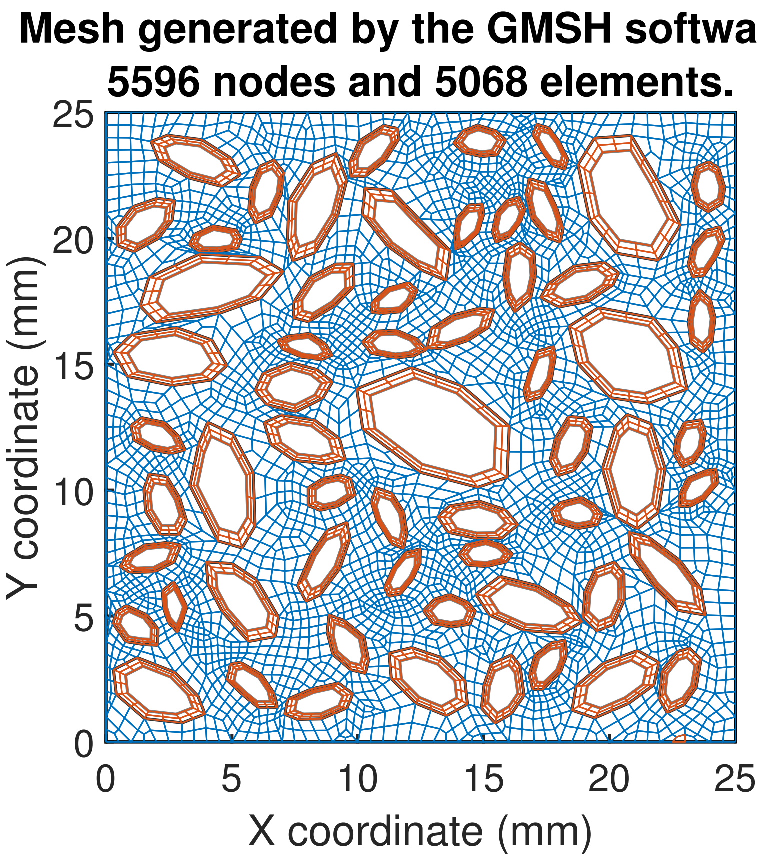

Figure 8: Example of a subscale representing a Recycled Aggregates Concrete for our multiscale numerical model. In blue, the new mortar, and in orange, the adherent mortar. Both may have distinct transfer properties. The natural aggregates, considered impervious with respect to mortar, are unmeshed.

A detailed review of the model is available in Fanara et al. (2024) [32]. The constitutive equations at both scales, as well as the algorithm to obtain the subscale, are presented. The parameters implemented in the model are all obtained from the experimental campaign and shown in Table 3.

4. Sensitivity Analysis on the Hysteresis

The implementation of the hysteresis of the water retention curve requires controlling several variables. These include the parameter b, which influences the gradient of the scanning curve [30], and the increment of suction ds, which may introduce estimation errors for

Table 3: Results of the experimental campaign for the three compositions studied: E-M, NAC and RAC.

Parameter	**E-M**	**NAC**	**RAC**
Water absorption experiment			
Dry Density [kg/m^3]	2025	2263	2061
Porosity [% Volume]	22.83	14.16	20.5
Water permeability experiment			
Intrinsic Permeability [10^{-19}m^2]	38.7	1.73	2.58
Static sorption and desorption experiment			
n_{vG} (Desorption) [-]	1.35	1.39	1.36
n_{vG} (Sorption) [-]	1.4	1.38	1.36
α_{vG} (Desorption) [MPa]	6.23	8.16	7.2
α_{vG} (Sorption) [MPa]	0.77	0.41	0.54
Hysteresis b_1 [-]	0.8	0.85	0.75
Hysteresis b_2 [-]	1.1	1.2	1.2
Diffusion under unsteady-state			
D_{app} [10^{-11}m^2/s at 29 days]	1.43	1.41	1.65

the slope of the scanning curve, as per Equation 8.

The first parameter is obtained experimentally by fitting, although sorption and desorption experiments can be slow and laborious, particularly when observing hysteresis. Additionally, the experimental work in this research has demonstrated that a single value of b may not satisfy the same material, depending on its history. Therefore, it is crucial to understand the effect of this parameter b on our model's response to characterise its significance.

The second variable, the increment of suction ds, varies in our simulation due to the applied boundary conditions. As per Equation 8, the derivative $\partial S_r/\partial_s$ is assumed constant over the increment of suction ds. The model is therefore more prone to error with larger increments, as this assumption only holds for small increments of suction.

The following two sections examine the impact of each variable. The model employs the parameters listed in Table 3. As the mesoscale is composed of permeable mortar, the implemented mesoscale properties (porosity, intrinsic permeability, and chloride diffusion coefficient) are those of the E-M composition, multiplied by 1.3 to account for the difference between a 2D and 3D model [32]. The water retention curve, however, is considered as a macroscale property. Indeed, the parameters of the WRC mainly depend on the type and size of the pores. In our multiscale model, such small components are not directly modelled, and a homogeneisation is thus necessary. Two options were available: define the WRC as mesoscale properties, and use the parameters related to the E-M, or define them as macroscale properties and use the parameters of the concretes directly. The second option was chosen as the first seemed to oversimplify the problem. Therefore, the parameters implemented for the WRC correspond to either NAC or RAC, depending on the mesoscale used. Figure 9 shows the two mesoscale representative volume elements modelled for the NAC and RAC used in this sensitivity analysis. The macroscale represents a 1D sample that is 10cm long (Figure 10).

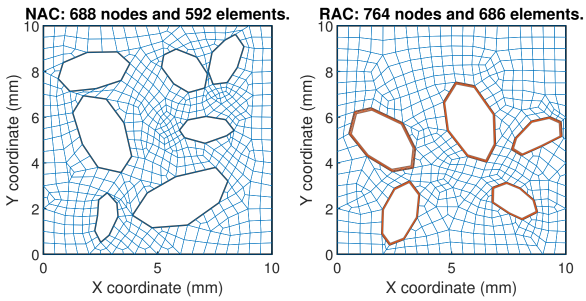

Figure 9: RVE representing the mesoscale of both NAC (left) and RAC (right), with properties of the E-M composition for the blue mortar phase (new mortar matrix) and the same properties for the orange mortar phase (adherent mortar of the RCA).

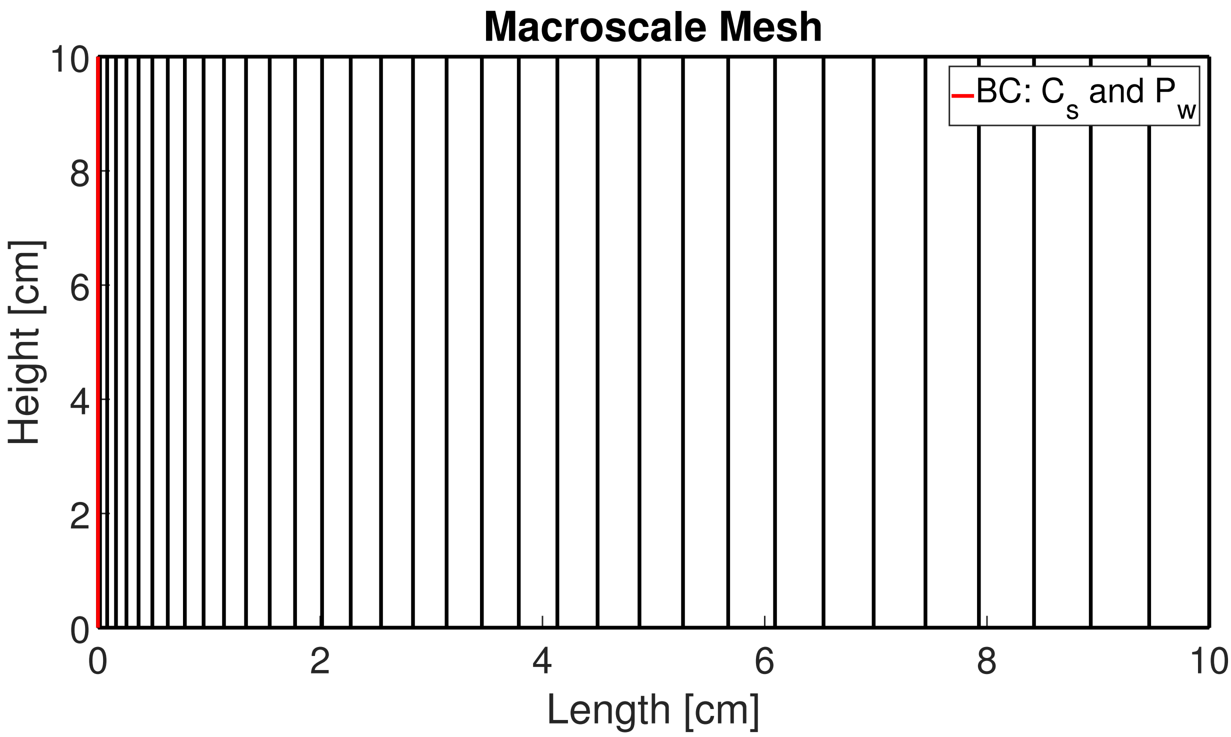

Figure 10: Macroscale mesh for the study of the influence of both the increment of suction and the parameter b on the hysteresis model.

4.1. Influence of the Increment of Suction

The first sensitivity analysis performed focuses on the increment of suction. A study was conducted using our multiscale model, and the results are presented in Figure 11. It displays the solutions of our model to three values of suction increment. Indeed, the increment of suction calculated from the boundary conditions is divided into sub-increments of equal value N. The variation in refinement results in a difference in the degree of saturation of the porous medium, even when the same final suction value is applied as a boundary condition. The degree of difference may be significant, depending on the size of sub-increments applied. The reason for this resides in the use of derivatives to navigate the scanning curves, which are supposed constant over the increment of suction ds. It was therefore chosen to relate the value of the sub-increment N to the air-entry pressure as it allows for precise results while maintaining a physical meaning.

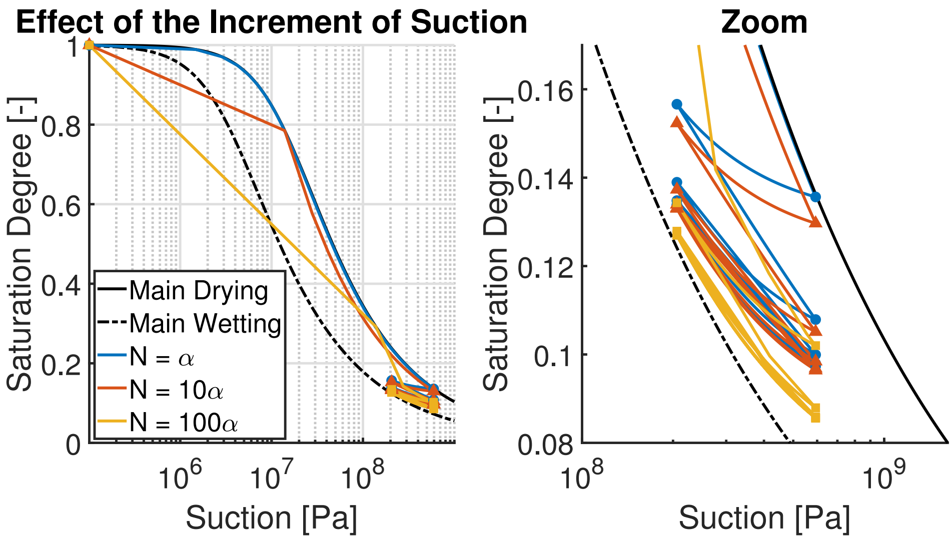

Figure 11: Effect of the increment of suction on the hysteresis model. On the left, the total response for three different values of increment of suction (noted N). On the right, a zoom on the hysteresis part of the response.

4.2. Influence of Parameter b

The second parameter studied is b, a positive, dimensionless value that controls the slope of the hysteresis scanning curve. This curve ranges from parallel to the main water retention curve (b closer to zero) to horizontal (b closer to infinity). Figure 13 displays the results of our multiscale model for a NAC and RAC RVE, and for various values of b. Two simulations were conducted without the hysteresis of the water retention curve, using properties of the boundary drying or wetting curves.

The initial water pressure conditions inside the sample were equal to the atmospheric pressure. The pressure on the outside border is changed bi-annually to -2MPa and -200MPa for a period of ten years. Furthermore, the outside border is set to have a chloride content of 0.11 [-], while the inside of the sample is initially devoid of chloride. The macroscale mesh and the boundary conditions are shown in Figures 10 and 12.

The higher the value of b, the faster the hysteresis reaches the boundary curves. Additionally, the saturation degree throughout the NAC has a greater variation range than the RAC RVE.

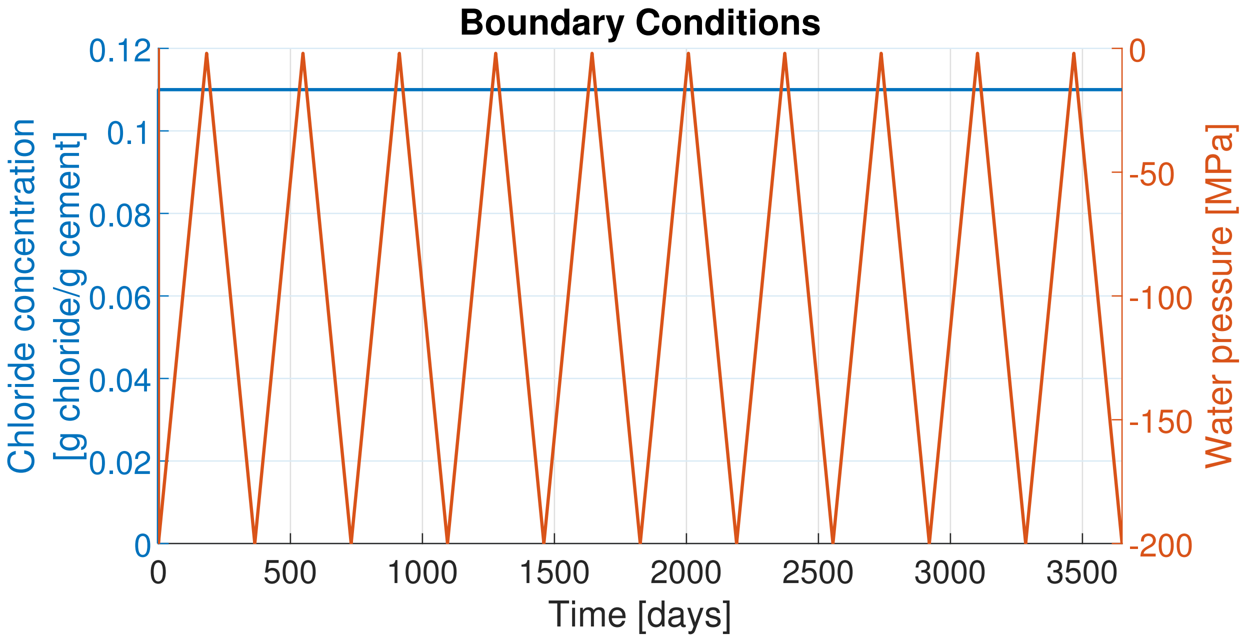

Figure 12: Boundary conditions for the study of the influence of the parameter b on the hysteresis model.

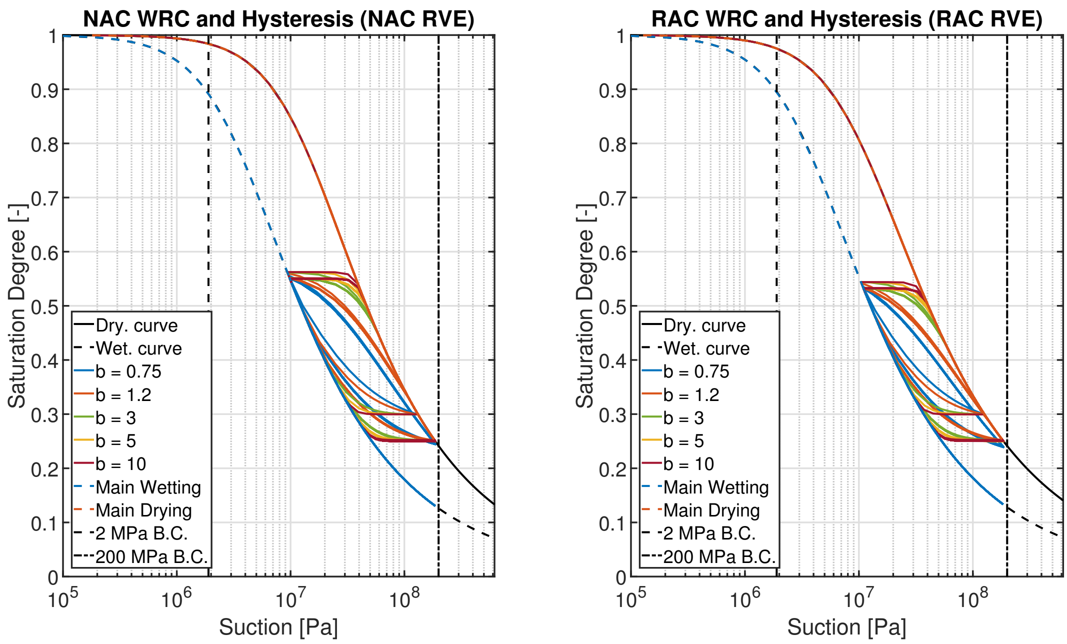

Figure 13: Influence of the parameter b on the hysteresis model: evolution of the saturation degree with the applied suction, for NAC (left) and RAC (right).

This is confirmed by Figure 14, which shows the evolution of the saturation degree at the surface of exchange of the concrete for both the NAC and RAC. It is evident that the hysteresis curves approach the main boundary curves during both drying and wetting phases. The transition slope becomes more horizontal with an increase in the value of b, which relates to a faster convergence of the hysteresis curves to the boundary curves.

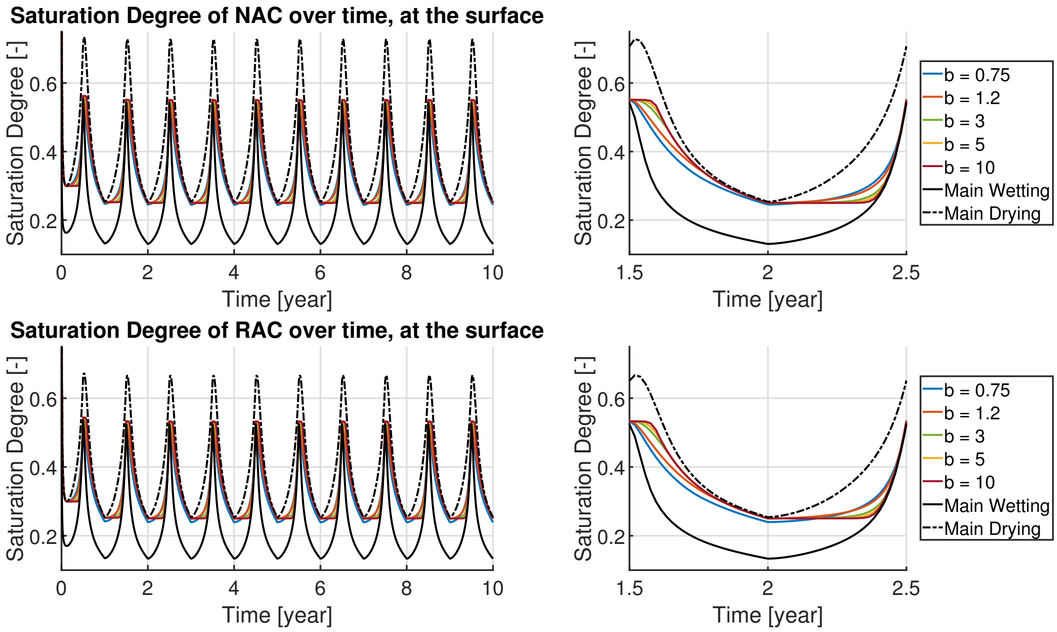

Figure 14: Influence of the parameter b on the hysteresis model: Water Saturation Degree of NAC and RAC at the surface over a ten-year period (left), with a focus on a specific year (right).

Figures 15 and 16 show the chloride content evolution at depths of 0cm, 2cm, 5cm, and 10cm inside the sample for both NAC and RAC over a ten-year period. Additionally, the results are presented in Figure 17 at a depth of 3cm only.

As the value of b increases, the variations between drying and wetting phases decrease and the water saturation degree evolves more linearly. Consequently, the chloride content tends to be higher for greater values of b, with a negligible difference for values of 3 and above. Using a higher value of b is therefore conservative due to the overestimation of the chloride content.

Furthermore, the impact of the boundary conditions is smaller at greater depth, the diffusion being predominant over the advection of chloride ions. At the surface, the difference between the values of b is negligible due to the applied boundary conditions.

Additionally, it may be concluded that higher saturation degrees and chloride contents are positively correlated, as supported by simulations without hysteresis. Indeed, the sample with the boundary drying curve consistently exhibits higher chloride content than the one with the boundary wetting curve.

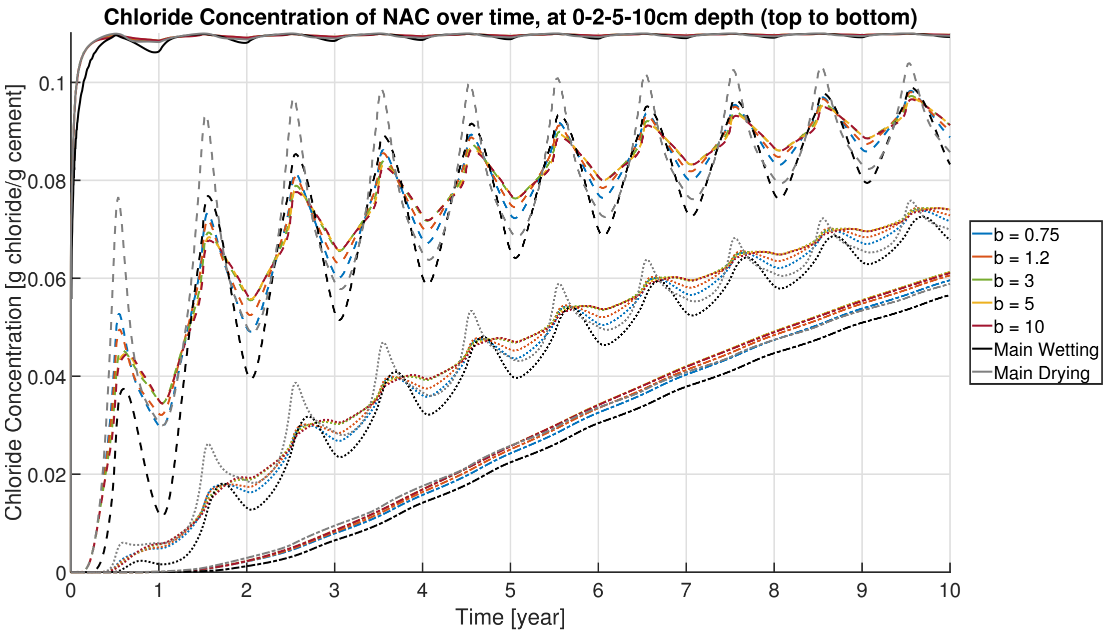

Figure 15: Influence of the parameter b on the hysteresis model: Chloride Content of NAC at 0, 2, 5 and 10cm depth over a ten-year period.

Therefore, it is necessary to implement the hysteresis model to obtain accurate chloride content values. Otherwise, the chloride content may be underestimated or overestimated when using the properties of the boundary wetting or drying curve, respectively. Additionally, it is useful to use the correct value of b, which can be obtained experimentally, to avoid overestimating the chloride content within the sample. However, if experimental work is to be excluded, a value of b greater than 3 should be used as it is on the safety side. Furthermore, the difference in chloride content caused by the different values of b decreases with time, as represented in Figures 18 and 19, which show the mean chloride content over

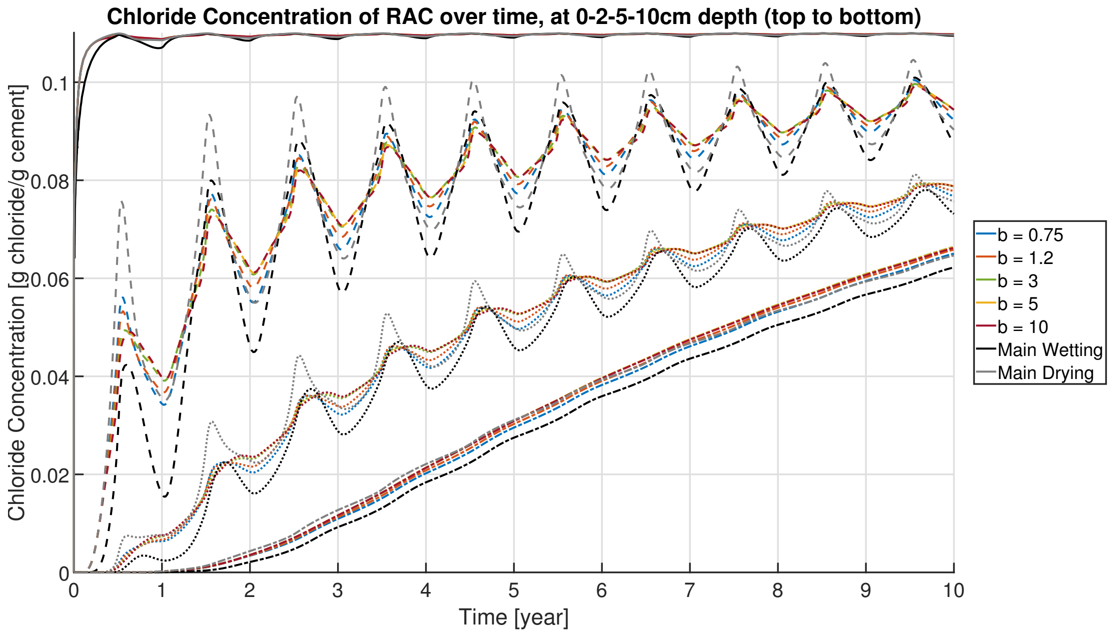

Figure 16: Influence of the parameter b on the hysteresis model: Chloride Content of RAC at 0, 2, 5 and 10cm depth over a ten-year period.

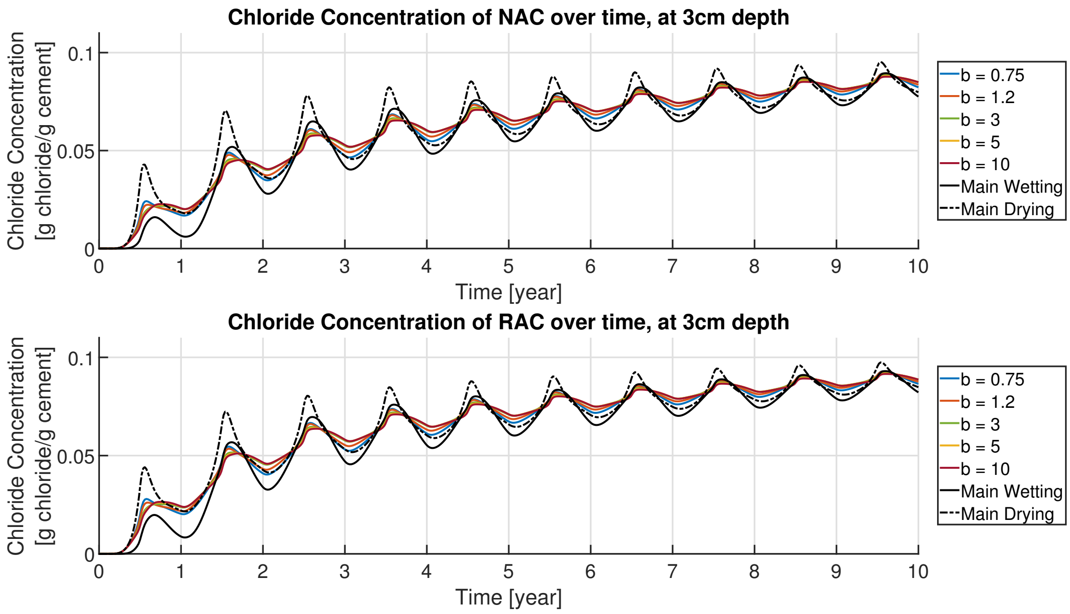

Figure 17: Influence of the parameter b on the hysteresis model: Chloride Content of NAC and RAC at 3cm depth over a ten-year period.

the first two centimetres of the sample, after 189 days and 10 years, respectively. One may see that after 189 days, there is a noticeable difference in between the several values of b. However, after 10 years, only a slight difference in the mean chloride content for the different values of b is visible. However, once again, the usefulness of the implementation of the hysteresis is confirmed as the results for the boundary curves only are quite different than with the hysteresis implemented.

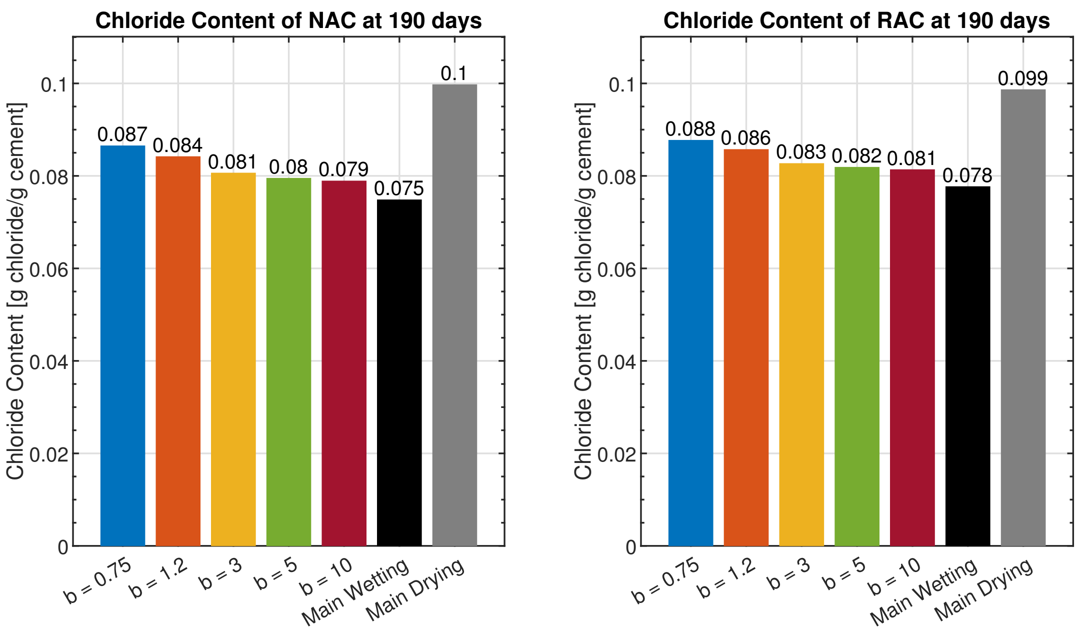

Figure 18: Influence of the parameter b on the hysteresis model: mean chloride content over the first 2cm of the sample, after 189 days.

5. Conclusion

This paper focuses on implementing a hysteresis model for the water retention curves of concrete. Water retention curves are a useful tool for modelling unsaturated conditions in porous materials. However, their hysteresis is often neglected when implemented numerically due to the difficulty of obtaining experimental results for calibration. For the development of this model, the Van Genuchten model (1980) [24] was implemented for the boundary drying and wetting curves, along with the hysteresis model by Zhou et al. (2012) [30] that

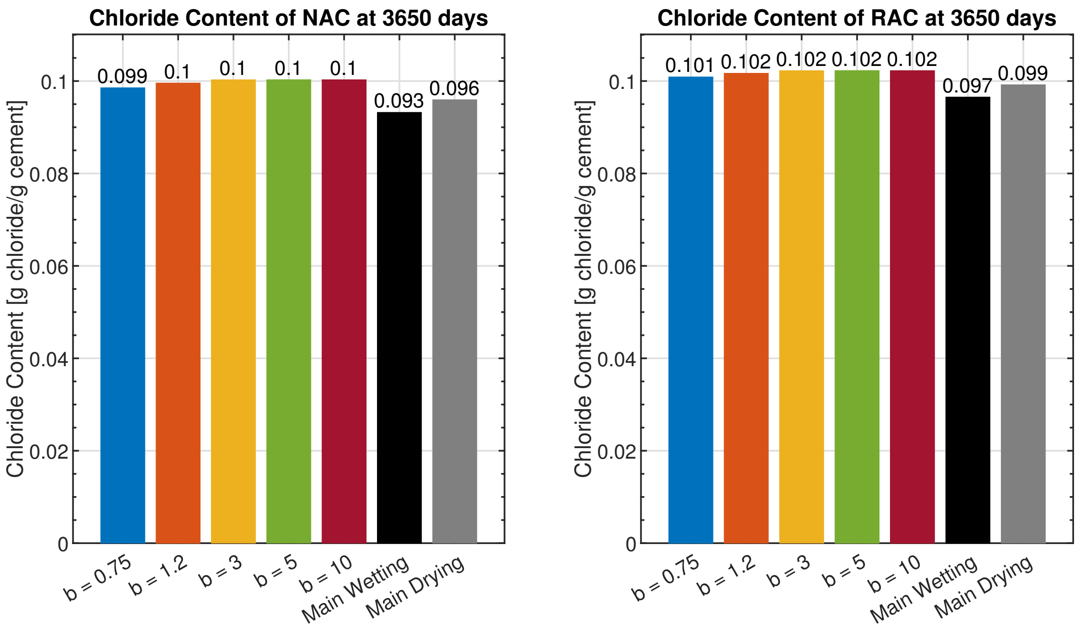

Figure 19: Influence of the parameter b on the hysteresis model: mean chloride content over the first 2cm of the sample, after 10 years.

is compatible with the boundary curves of Van Genuchten.
Experiments were conducted on concretes made of 100% natural aggregates and recycled concrete aggregates, as well as on an equivalent mortar. This experimentation allowed for the determination of numerous parameters necessary for the implemented constitutive equations. The Van Genuchten model, along with the hysteresis model by Zhou et al., was experimentally calibrated to accurately replicate unsaturated conditions of concrete made from natural or recycled aggregates.

The model was used for a sensitivity analysis on two parameters: the value of b, the fitting parameter for the hysteresis model, and the increment of suction ds (Equation 8). It was necessary to perform experiments to calibrate the value of parameter b as the saturation degree obtained numerically may be erroneous. To better understand the influence of b, the model allowed for the ingress of chloride ions into the concrete. Chloride ingress is strongly influenced by the saturation degree of the porous system, making it a useful tool for characterising the impact of the hysteresis. Results have shown that higher values of b correspond to higher chloride content. Therefore, it may be better to use a value of b of 3 or higher to err on the side of caution and avoid the need for further experimentation. Regarding the increment of suction (ds), it has been proven to significantly affect the saturation degree as per Equation 8. Therefore, it was decided to divise the boundary conditions into sub-increments whose value is equal to the air-entry pressure, which has proven to be sufficient for obtaining accurate results.

When comparing the results of our study between the NAC and RAC, it was experimentally found that the RAC has a smaller (or higher) air-entry pressure for the boundary drying (or wetting) curve. This means that the exchange of moisture with the environment takes place sooner than for the NAC. The parameter n_{vG}, which corresponds to the rate of (de)saturation, is rather similar for both compositions. If we consider the chloride content of the two compositions, the chloride content of the RAC tends to be higher than that of the NAC, which is logical because of the greater movement of water between the sample and its environment, and the greater chloride diffusion coefficient of the RAC.

Acknowledgements

Funding: This work is supported by the Wallonia regional government (Belgium) in the framework of a FRIA (Fund for Industrial and Agricultural Research) grant.

Competing Interests

The authors declare that they have no known competing financial interests or personal relationships that could have appeared to influence the work reported in this paper.

References

[1] C. S. Rangel, M. Amario, M. Pepe, E. Martinelli, R. D. Toledo Filho, Influence of Wetting and Drying Cycles on Physical and Mechanical Behavior of Recycled Aggregate Concrete, Materials 13 (2020) 5675.

[2] R. A. Patel, P. Janez, J. Diederik, Multi-scale modeling strategies to improve durability models for service life predictions of concrete structures, in: G. D. Schutter, N. D. Belie, A. Janssens, N. V. D. Bossche (Eds.), XIV DBMC - 14th International Conference on Durability of Building Materials and Components, RILEM, Ghent University, Belgium, pp. 309–310.

[3] P. S. Mangat, B. T. Molloy, Prediction of long term chloride concentration in concrete, Materials and Structures 27 (1994) 338–346.

[4] M. Morga, G. C. Marano, Chloride Penetration in Circular Concrete Columns, International Journal of Concrete Structures and Materials 9 (2015) 173–183.

[5] I. Balafas, C. J. Burgoyne, Environmental effects on cover cracking due to corrosion, Cement and Concrete Research 40 (2010) 1429–1440.

[6] A. Rao, K. N. Jha, S. Misra, Use of aggregates from recycled construction and demolition waste in concrete, Resources, Conservation and Recycling 50 (2007) 71–87.

[7] F. Debieb, L. Courard, S. Kenai, R. Degeimbre, Mechanical and durability properties of concrete using contaminated recycled aggregates, Cement & Concrete Composites 32 (2010) 421–426.

[8] A. Fanara, L. Courard, F. Collin, J. Hubert, Transfer properties in recycled aggregates concrete: Experimental and numerical approaches, Construction and Building Materials 326 (2022) 126778.

[9] J. Bear, A. Verruijt, Modeling Groundwater Flow and Pollution, D. Reidel Publishing Company, 1987.

[10] H. Q. Pham, D. G. Fredlund, S. L. Barbour, A study of hysteresis models for soil-water characteristic curves, Canadian Geotechnical Journal 42 (2005) 1548–1568.

[11] M. Nuth, L. Laloui, Advances in modelling hysteretic water retention curve in deformable soils, Computers and Geotechnics 35 (2008) 835–844.

[12] C. T. Beckett, C. E. Augarde, Prediction of soil water retention properties using pore-size distribution and porosity, Canadian Geotechnical Journal 50 (2013) 435–450.

[13] M. Pap, A. Mahler, S. G. Nehme, Measurement of water retention curve for different concrete mixtures, 2018.

[14] R. M. Bowen, Incompressible porous media models by use of the theory of mixtures, International Journal of Engineering Science 18 (1980) 1129–1148.

[15] F. A. Concha, Solid-Liquid Separation in the Mining Industry, volume Fluid Mechanics and Its Applications (Book 105), Springer International Publishing Switzerland, 2014.

[16] M. Pap, A. Mahler, S. G. Nehme, Analysis and Finite Element Modelling of Water Flow in Concrete, Periodica Polytechnica Civil Engineering (2018).

[17] D. G. Fredlund, D. Sheng, J. Zhao, Estimation of soil suction from the soil-water characteristic curve, Canadian Geotechnical Journal 48 (2011) 186–198.

[18] J. Hubert, Experimental and numerical study of cracking during the drying of porous materials :

application to the fields of chemical engineering and geomechanics, Ph.D. thesis, ULiège University, 2018.

[19] W. J. Likos, N. Lu, J. W. Godt, Hysteresis and Uncertainty in Soil Water-Retention Curve Parameters, Journal of Geotechnical and Geoenvironmental Engineering 140 (2014).

[20] G. Capparelli, G. Spolverino, An Empirical Approach for Modeling Hysteresis Behavior of Pyroclastic Soils, Hydrology 7 (2020) 14.

[21] J. Simunek, R. Kodesova, M. M. Gribb, M. T. van Genuchten, Estimating hysteresis in the soil water retention function from cone permeameter experiments, Water Resources Research 35 (1999) 1329–1345.

[22] F. Abbasi, M. Javaux, M. Vanclooster, J. Feyen, Estimating hysteresis in the soil water retention curve from monolith experiments, Geoderma 189–190 (2012) 480–490.

[23] Y. Kohgo, A Hysteresis Model of Soil Water Retention Curves Based on Bounding Surface Concept, Soils and Foundations 48 (2008) 633–640.

[24] M. T. Van Genuchten, A Closed-form Equation for Predicting the Hydraulic Conductivity of Unsaturated Soils, Soil Science Society of America Journal 44 (1980) 892:898.

[25] J. Hubert, Z. Zhao, F. Michel, L. Courard, Effect of crushing method on the properties of produced recycled concrete aggregates, Buildings 13 (2023) 2217.

[26] A. Schwartzentruber, C. Catherine, La méthode du mortier de béton équivalent (MBE) - Un nouvel outil d'aide à la formulation des bétons adjuvantés, Materials and Structures 33 (2000) 475–482.

[27] A. Fanara, L. Courard, F. Collin, Numerical and experimental study of chloride ion transport in recycled aggregates concrete, Academic Journal of Civil Engineering 40 (2023) Vol 40 No 2 (2022): Special Issue–NoMaD 2022.

[28] S. J. Kowalski, Thermomechanics of Drying Processes, Springer-Verlag Berlin Heidelberg GmbH, 2003.

[29] P. Delage, M. Howat, Y. Cui, The relationship between suction and swelling properties in a heavily compacted unsaturated clay, Engineering Geology 50 (1998) 31–48.

[30] A.-N. Zhou, D. Sheng, S. W. Sloan, A. Gens, Interpretation of unsaturated soil behaviour in the stress – Saturation space, I: Volume change and water retention behaviour, Computers and Geotechnics 43 (2012) 178–187.

[31] F. Collin, X. Li, J. Radu, R. Charlier, Thermo-hydro-mechanical coupling in clay barriers, Engineering Geology 64 (2002) 179–193.

[32] A. Fanara, L. Courard, F. Collin, Numerical FE^2 study of chloride ingress in unsaturated recycled aggregates concrete, Cement and Concrete Research 186 (2024) 107703.